www.lajss.org
Latin American Journal of Solids and Structures 1 (2004) 169–184

Topology optimization of multiple physics problems modelled by Poisson's equation

Alberto Donoso[a] and Ole Sigmund[b,*]

[a]Departamento de Matemáticas, ETSI Industriales
Universidad de Castilla- La Mancha, 13071
Ciudad Real, Spain
[b]Department of Solid Mechanics, Building 404
Technical University of Denmark
DK-2800 Lyngby, Denmark

Abstract

In this paper we apply topology optimization to analyse multiple physics design problems which are modelled by Poisson's equation. Since the governing differential equation has the same format in all situations, we can solve a number of different physics problems, simply by choosing the variables properly and choosing the appropriate boundary conditions in each case. We treat both the minimum energy case as well as "mechanisms design" problems, i.e., for given input, minimize (or maximize) response by the state or the gradient in other parts of the structure.

Keywords: Optimized design, topology optimization, conduction, Poisson's equation

1 Introduction

There exist several physical phenomena which can be described by the same form of differential equation that explains conduction in heat transfer [6]. For simplicity, we specialize conditions to time-independence and the two-dimensional case. Consider the following governing differential equation

$$-\mathrm{div}(k\nabla u) = Q.$$

In the heat transfer case, the solution of the state equation is a scalar function, $u = u(x_1, x_2)$, which represents the temperature, k is the thermal conductivity and Q is the rate of internal heat generation per unit volume.

By changing the meaning of the state, u, the material property, k, and the source term of the equilibrium equation, Q, and also using the appropriate boundary conditions in each case, we can described different phenomena in multiple physics contexts such as groundwater flow and plane

* Corresponding author Email: sigmund@mek.dtu.dk Received 27 Feb 2004; In revised form 16 March 2003

Table 1: Meaning of different components of Poisson's equation.

Poisson's equation			
Physics	u	k	Q
heat conduction	temperature	thermal conductivity	heat generation
groundwater flow	hydraulic head	permeability	0
potential flow	potential function	1	0
elastic torsion	stress function	shear modulus^{-1}	twist angle
pressurized membrane	lateral deflection	surface tension	lateral pressure
electrostatics	voltage	permittivity	charge density
magnetostatics	magnetic vector	medium's response	current density
diffusion	diffusion constant	moisture concentration	production rate

incompressible irrotational flow in fluid mechanics, elastic torsion and pressurized membranes in solids mechanics and also situations in electrostatics and magnetostatics (see Table 1). Finally, we should interpret the results depending on the physical situation.

To fix ideas and explain our aim, we begin considering the context of heat transfer. In a general way, the problem we would like to solve consist of determining how we have to place fixed amounts of two isotropic materials with different thermal conductivities, α and β, $0 < \alpha < \beta$, so as to minimize (or maximize) a desired property (given by the $g(\rho, u)$ function) in the thermal device occupying the design domain.

Let us denote by (P) the problem

$$\text{Minimize (or Maximize):} \quad c(\rho) = g(\rho, u),$$

subject to

$$-\text{div}(k(x)\nabla u(x)) = Q(x), \quad \text{in } \Omega,$$
$$-k(x)\nabla u(x) \cdot n = f(x), \quad \text{on } \Gamma_t,$$
$$u = u_0, \quad \text{on } \Gamma_0,$$
$$k(x) = \beta\rho(x) + \alpha(1 - \rho(x)),$$
$$\frac{1}{|\Omega|}\int_\Omega \rho(x)\, dx \leq V, \quad 0 < V < 1.$$

Typically, the characteristic function ρ indicates where the β-material is to be placed and V is the relative volume fraction of the β-material, which is given.

It is well-known that such problems lack optimal solutions within the class of characteristic functions. This kind of problems are ill-posed in the sense that one generally can find a finer and more detailed material distribution that is better than the coarser design, it is called mesh-dependence. Ways to circumvent the ill-posedness problem are reviewed in [15] and can be divided into two groups, namely relaxation methods and restriction methods. The former expands the design space by introducing an infinitely fine microstructure as material properties in every element of the structure, see in detail [2]. Using this approach results in structures with large "grey regions" ($0 < \rho < 1$), which are very difficult to manufacture. On the other hand, restriction methods introduce extra constraints on design variables so as to find optimized solutions over the initial design space. One of these, used here, is a filtering technique which modifies the design sensitivity of an specific element based on a weighted average of the element sensitivities in a fixed neighborhood, see [15]. The trouble is now how to solve the resulting discrete problem, having in mind that as finer meshes are used, the number of design variables is larger and therefore, the number of material distribution combinations increases in an astronomical way. One popular way is to convert the discrete problem into a continuous one by allowing intermediate densities during the optimization process. By penalization schemes, these intermediate densities are then forced towards discrete 0/1 solutions at the end of the optimization process. This continuous-variable scheme is the power-law approach to topology optimization, also called SIMP (Solid Isotropic Material with Penalization [1]), and for the two-material problem, the model can be expressed as

$$k(x) = \beta\rho(x)^p + \alpha(1 - \rho(x)^p),$$

where p is the penalty factor. The volume constraint is now given by

$$\frac{1}{|\Omega|}\int_\Omega \rho(x)\, dx \leq V, \quad 0 \leq \rho(x) \leq 1.$$

By selecting the value of the power, p, large enough (usually larger than 3, (see [3])), elements with intermediate densities become inefficient (when a volume constraint is present, like now) and are thus forced towards zero or one. The power-law approach to topology optimization has been applied to problems with multiple constraints, multiple physics and multiple materials, in all of them successfully (see for example [14]).

Previous works have appeared on the applications of the topology optimization method to problems modelled by Poisson's equation, where the objective function mainly has been of energy form (for conduction problems see [4, 7, 9, 12] and for torsion problems see [5, 8, 10, 11]). In this paper, we repeat some of the old examples and extend the ideas to non-energy (mechanism-type) problems. In particular we consider problems in conduction, ground-water flow, pressurized membranes and elastic torsion. The examples offer new physical insight in the various optimization problems.

2 Numerical implementation

The implementation of the topology optimization problem is straight-forward and follows the usual procedure outlined in the references on topology optimization, see [13]. The standard procedure is to consider the design problem as an optimization problem in the design variables, $\rho(x)$, only. The displacement field is regarded as a function of these design variables through the equilibrium equation. To start with, we take an initial design which satisfies the volume constraint, e.g., homogenous distribution of material. Next we compute the displacement field by using FE analysis (in this case, we have used square elements with Q4 interpolation of displacements and element-wise constant densities),

$$\mathbf{K}\mathbf{u} = \mathbf{f}.$$

Later we have to find the derivatives of the objective function with respect to the design variables by using the adjoint method, it is called the sensitivity analysis,

$$\frac{\partial c}{\partial \rho_e} = \frac{\partial g}{\partial \rho_e}\mathbf{u} + \mathbf{p}^T \frac{\partial \mathbf{K}}{\partial \rho_e}\mathbf{u},$$

where

$$\mathbf{K}\mathbf{p} = -\frac{\partial g}{\partial \mathbf{u}}.$$

For the compliance case we can use an optimality criteria method to solve the optimization problem but when we consider non-self-adjoint problems, sensitivities may take both positive and negative values, resulting in ill-convergence of the simple optimality criteria approach. In such cases the best convergence is obtained using a mathematical programming algorithm like MMA (see [16]).

3 Numerical examples

3.1 Heat transfer

As we presented before, the design problem for the heat transfer situation would show the following format:

$$\text{Minimize (or Maximize):} \quad c(\rho) = g(\rho, u),$$

subject to

$$-\text{div}(k(x)\nabla u(x)) = Q(x), \quad \text{in } \Omega,$$

$$-k(x)\nabla u(x) \cdot n = f(x), \quad \text{on } \Gamma_t,$$

$$u = u_0, \quad \text{on } \Gamma_0,$$

$$k(x) = \beta\rho(x) + \alpha(1 - \rho(x)),$$

$$\frac{1}{|\Omega|}\int_\Omega \rho(x)\, dx \leq V, \quad 0 < V < 1.$$

Concerning this case study, in all examples the design domain is a square and the material properties take the values $\beta = 1$ (good conductor) and $\alpha = 0.001$ (bad conductor or insulator). In the first example the design domain (see Figure 1(a)) is isolated ($f = 0$) except for a small sink ($u_0 = 0$) in the middle of the left side. Under an uniform heat generation over all the domain ($Q = 1$), we want to find the optimized layout which minimizes the dissipated energy in the thermal device, so in this case the objective function is the compliance, $g_1(u) = Qu$. We have constrained the amount of β to be 40% (it corresponds to taking $V = 0.4$). A gray scale has been used to represent the optimized solution (see Figure 1(b)), where black would correspond to the β-material and white to the α-material. This optimized solution has already been obtained before in [4, 9]. We see how the good conductor (black material) drains energy away from all parts of the structure.

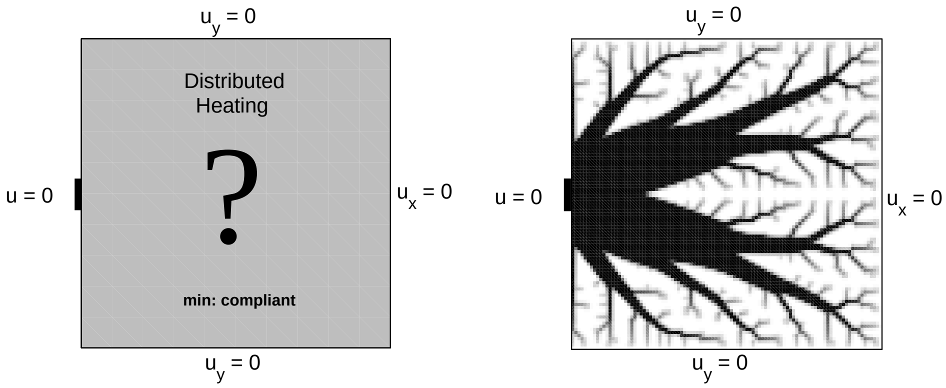

(a) Design domain (b) Optimized design

Figure 1: Optimized solution for Example 1

In the second example, we use the same design domain than before, but we are now interested in maximizing the outward horizontal heat flux in a small area as close as possible to the sink (see Figure 2(a)). In such a case, the objective function would be given by $g_2(\rho, u) = (k(\rho)u_{x_1})_{out}$[1]. The optimized design for $V = 0.4$ is shown in Figure 2(b) together with a plot of the heat flux in Figure 2(c). The intricate resulting topology can be interpreted as the design that for a limited amount of conducting material seeks to drain the energy close to the sink and direct it horizontally towards the sink.

In the last two examples of this section the boundary conditions are different (see Figures 3(a) and 4(a)). The distributed heating from before is exchanged (now $Q = 0$) with an inward horizontal heat flux in the middle of the left side ($f = f_{in}$) and the sink is now in the center of the opposite side. We look for designs which maximize the heat flux and the temperature gradient, in the directions marked in the design domains (Figures 3(a) and 4(a)) over small centered areas. The objective functions would be, $g_3(\rho, u) = (k(\rho)u_{x_1})_{out}$ and $g_4(u) = (u_{x_1})_{out}$, respectively. The resulting designs for $V = 0.25$ are shown in Figures 3(b) and 4(b). As we can see in Figure 4(b), the bad conductor must be placed where a big temperature gradient is

[1]The pair of variables (x_1, x_2) appearing in the text correspond to the pair (x, y) in the pictures.

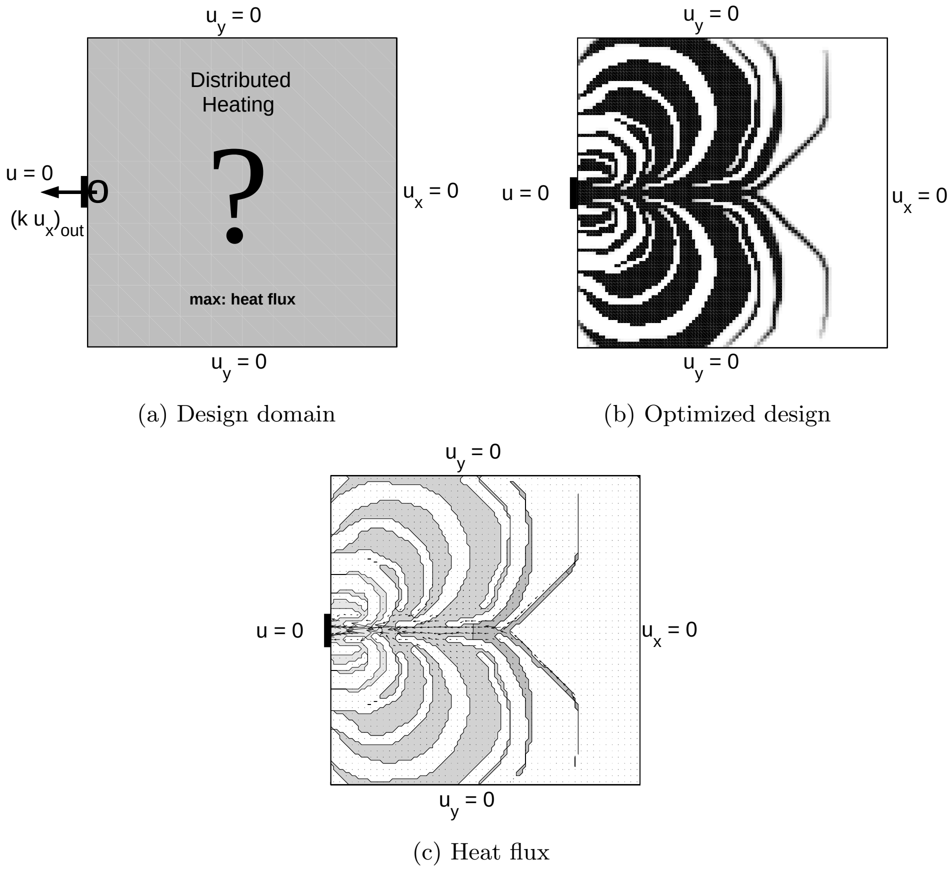

Figure 2: Optimized solution and field for Example 2

desired. Notice that if the α-material is a perfect insulator there is no energy transfer between the two branches appeared in the optimized design.

In Figures 5(a) and 5(b) the arrows represent the heat flux field and the intermediate shades are showing how the temperature is changing through the optimized design (dark zones are corresponding to higher temperature values).

3.2 Fluid mechanics

In fluid mechanics the groundwater flow design problem would adopt the following form

$$\text{Minimize (or Maximize):} \quad c(\rho) = g(\rho, p),$$

subject to

$$-\text{div}(k(x)\nabla p(x)) = 0, \quad \text{in } \Omega,$$

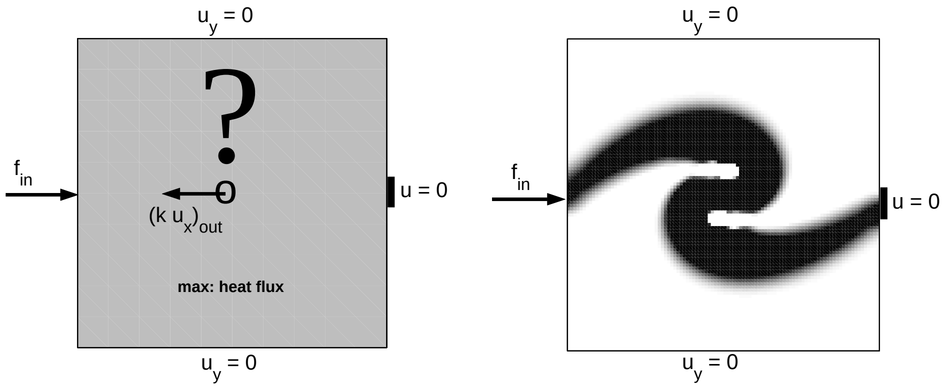

(a) Design domain (b) Optimized design

Figure 3: Optimized solution of Example 3

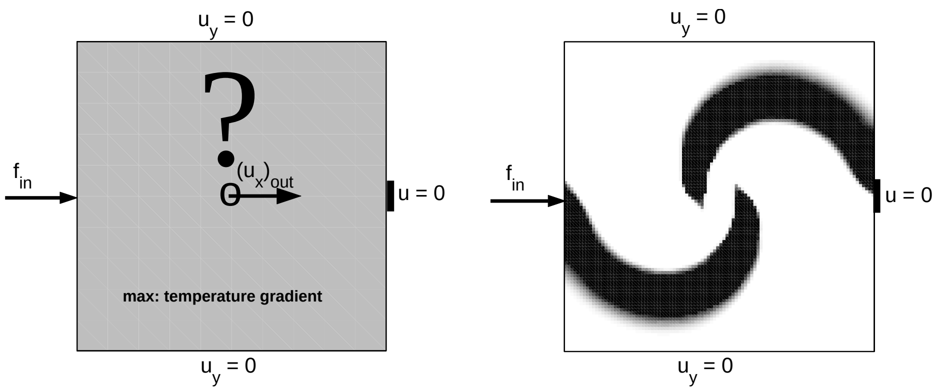

(a) Design domain (b) Optimized design

Figure 4: Optimized solution of Example 4

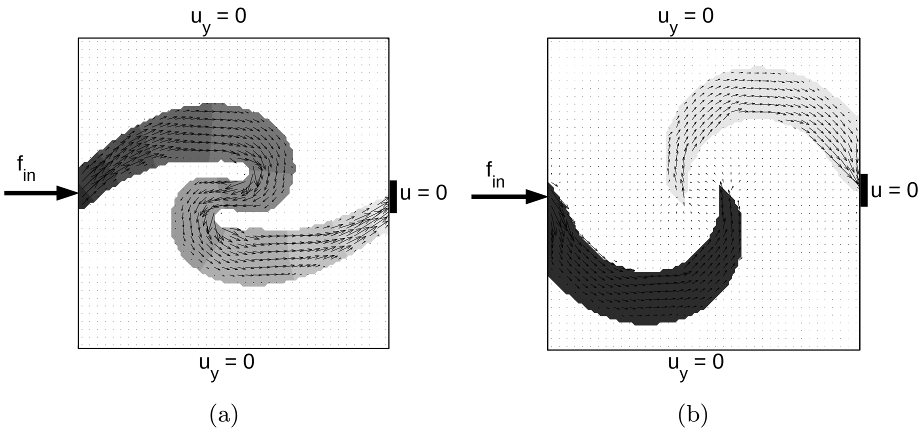

Figure 5: Heat flux for designs from Example 3 and 4

$$-k(x)\nabla p(x)\cdot n = u(x), \quad \text{on } \Gamma_t,$$

$$p = p_0, \quad \text{on } \Gamma_0,$$

$$k(x) = \beta\rho(x) + \alpha(1-\rho(x)),$$

$$\frac{1}{|\Omega|}\int_\Omega \rho(x)\, dx \le V, \quad 0 < V < 1.$$

In this new situation, the state is given by p (pressure), k means the hydraulic conductivity (or permeability) and it is common to take $Q \equiv 0$ and also work with the velocity field, u.

We will treat two cases, both of them with rectangular domains. In the first example, given an input flow on the left side ($u = u_{in}$) and a sink on the opposite side ($p_0 = 0$) and having in mind that the vertical component of the velocity in the other sides is zero (there is no vertical pressure gradient, see Figure 6), we want to find the optimized shape of an obstacle (it could be a pillar) so as to maximize the flow compliance (or minimize the dissipated energy). In this case, the objective function is the compliance, given by $g_1(p) = u_{in}p$). There exist two passive areas in the domain in order to reproduce the fact that there has to be fluid in both sides of the obstacle. Therefore, material properties are given by $\beta = 1$ (fluid) and $\alpha = 0.001$ (obstacle). The optimized solution for $V = 0.8$ is shown in Figure 7(a). Iso-pressure lines and the flow field are shown in Figure 7(b). As before, dark zones are corresponding to higher state (pressure) values.

In the second example, the design domain is the same but the objective consists of maximizing the flow velocity in the direction marked with an arrow in Figure 8. The function would be now $g_2(\rho,p) = u_{out} = (-k(\rho)\nabla p\cdot n)_{out} = \frac{\sqrt{2}}{2}(k(\rho)(p_{x_2} - p_{x_1}))_{out}$. The optimized solution for $V = 0.05$ is given by a centered slanted channel, as we can see in Figure 9(a). In Figure 9(b), a detailed picture about the flow field in a small centered area is shown.

3.3 Pressurized membranes

In the context of pressurized membranes the design problem would be given by

$$\text{Minimize:} \quad c(\rho) = g(\rho, u),$$

subject to

$$-\text{div}(s(x)\nabla u(x)) = P, \quad \text{in } \Omega,$$
$$u = 0, \quad \text{on } \partial\Omega,$$
$$s(x) = \beta\rho(x) + \alpha(1 - \rho(x)),$$
$$\frac{1}{|\Omega|}\int_\Omega \rho(x)\, dx \le V, \quad 0 < V < 1.$$

In this new case study, the state is given again by u, but now it is indicating the vertical displacement, s means the surface tension (proportional to material stiffness) and the source term is usually given by an uniform pressure, P. We have taken the values $\beta = 1$ (high surface tension) and $\alpha = 0.001$ (low surface tension).

We will consider two cases, both of them square domains clamped on all boundary (the vertical displacement is zero, $u = 0$). In the first example, (see Figure 10(a)), we look for minimizing the compliance ($g_1(u) = Pu$) and in the second one (Figure 11(a)), minimizing the deflection in the middle point of the membrane ($g_2(u) = u_{out}$). Optimized solutions for $V = 0.4$ and $V = 0.25$ are shown in Figures 10(b) and 11(b), respectively. In Figures 10(c) and 11(c), the lateral deflection is also shown for each case. It is interesting to note how in the first case, all the membrane deflections are limited, whereas in the second case, only the central part has limited deflections whereas the outer parts of the four quadrants are allowed to deflect badly.

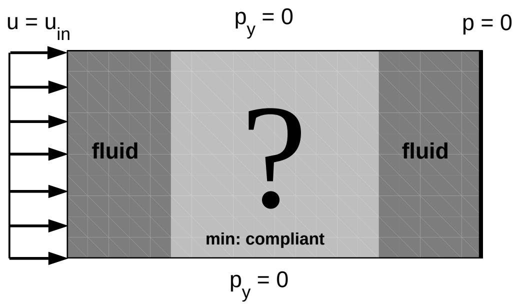

Figure 6: Design domain of Example 5

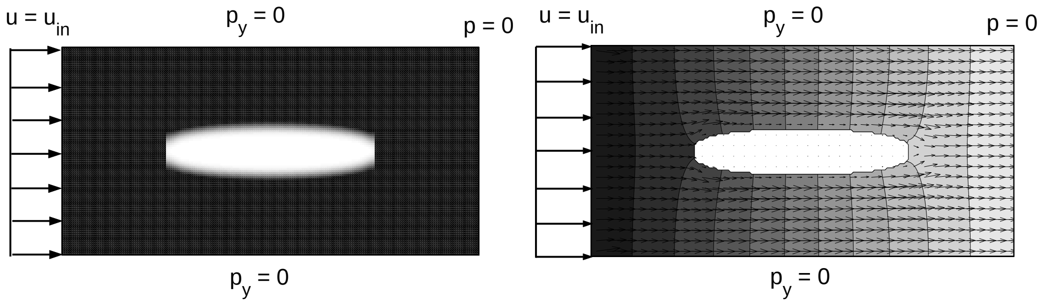

(a) Optimized design (b) Flow field

Figure 7: Optimized solution and field of Example 5

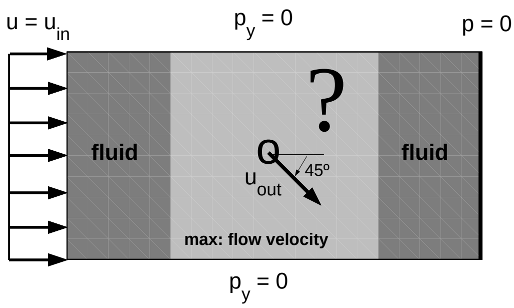

Figure 8: Design domain of Example 6

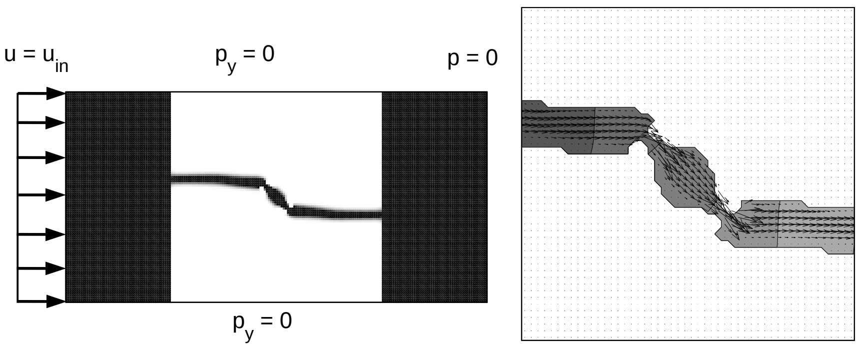

(a) Optimized design (b) Flow field

Figure 9: Optimized solution and field of Example 6

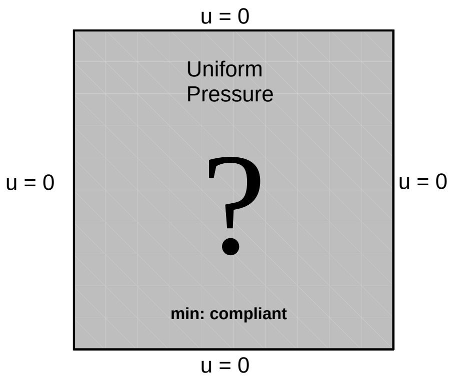

(a) Design domain

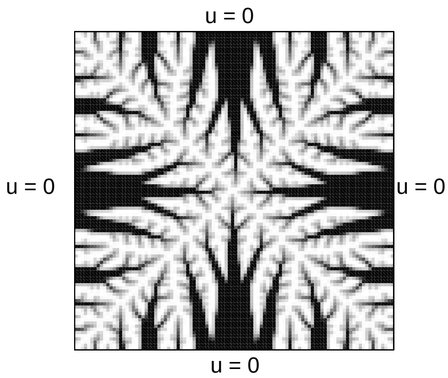

(b) Optimized design

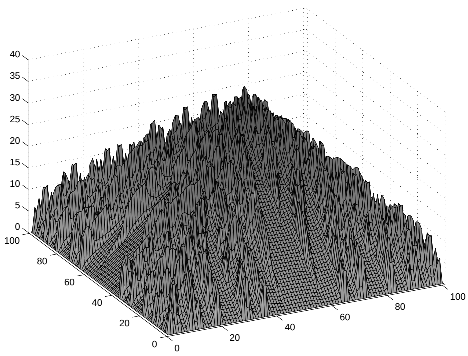

(c) Lateral deflection

Figure 10: Optimized solution of Example 7

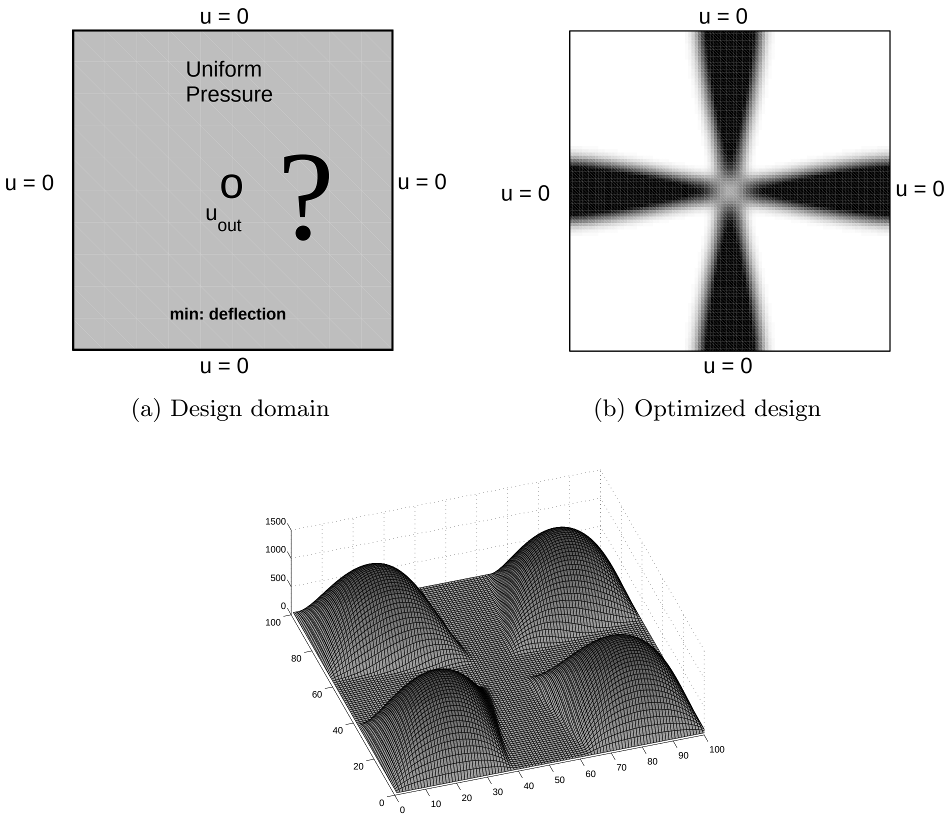

(a) Design domain

(b) Optimized design

(c) Lateral deflection

Figure 11: Optimized solution of Example 8

3.4 Elastic torsion

In the context of elastic torsion the design problem formulated in terms of the Prandtl or stress function would adopt the following form

$$\text{Minimize (or Maximize):} \quad c(\rho) = g(\rho, \phi),$$

subject to

$$-\text{div}\left(\frac{1}{G(x)}\nabla\phi(x)\right) = 2\theta, \quad \text{in } \Omega,$$
$$\phi = 0, \quad \text{on } \partial\Omega,$$
$$G(x) = \beta\rho(x) + \alpha(1-\rho(x)),$$
$$\frac{1}{|\Omega|}\int_\Omega \rho(x)\, dx \le V, \quad 0 < V < 1,$$

where the state is given by the stress function ϕ, the material properties are given by the shear modulus G, and the source term is an uniform twist angle θ. We will analyse three cases, in all of them the section of the elastic rod considered is a square. The fact that there is no normal stress along the boundary make us take $\phi = 0$ on $\partial\Omega$. The first situation corresponds to maximizing the torsion constant under an uniform twist angle ($\theta = 1$), (see Figure 12(a)). Thus, the objective function is the compliance and it is expressed as $g_1(\phi) = \frac{\phi}{\theta}$. The material properties take the values $\beta = 1$ (material) and $\alpha = 0.001$ (void). As we could have predicted and it is shown in Figure 12(b), the optimized solution for $V = 0.5$ corresponds, more or less, to placing the stiffer material in an outer concentric disk. Very similar results have been observed in the references [5, 8, 10, 11].

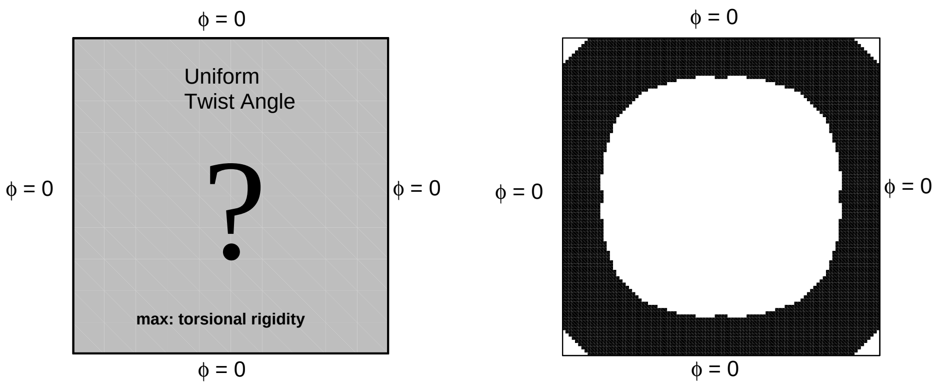

(a) Design domain (b) Optimized design

Figure 12: Optimized solution of Example 9

For the last two examples, we consider the design domain in Figure 13. The aim is to produce a maximum warp mechanism. The objective function consist of maximizing the difference between the vertical displacements, first when we consider the points A and B and second when they are C and D. The difference in displacements can be measured as the gradient of the vertical displacement function, w between the two points. Having in mind that

$$\frac{1}{G(x)}\nabla\phi(x) = \theta P + T\nabla w(x),$$

where

$$P = \begin{pmatrix} x_1 \\ x_2 \end{pmatrix}, \quad T = \begin{pmatrix} 0 & -1 \\ 1 & 0 \end{pmatrix},$$

it is not hard to realize that the objective functions for these two cases are given by $g_2(\rho,\phi) = (w_{x_1})_{AB} = (G(\rho)^{-1}(\phi_y))_{AB}$ and $g_2(\rho,\phi) = (w_{x_1})_{CD} = (G(\rho)^{-1}(\phi_y))_{CD}$.

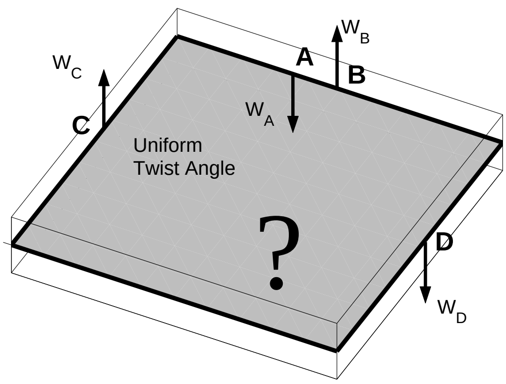

Figure 13: Design domain of Example 10 and 11

The optimized designs for $V = 0.15$ and $V = 0.05$ are shown in Figures 14(a) and 15(a), respectively. In Figures 14(b) and 15(b) the vertical displacement function, also called warping function, is shown for each case. Notice that, judging by the design in Figure 15(a), only the warping function along the $CDEF$ outline must be considered. We see that the maximum warping cross-section is obtained for open cross-sections with the material distributed as far away from the center axis as possible.

4 Conclusions

In this paper we have used the topology optimization method to study a range of new non-self-adjoint problems modelled by the Poisson's equation. A number of examples have been shown that offer new insight into optimal structural and multiple physics design.

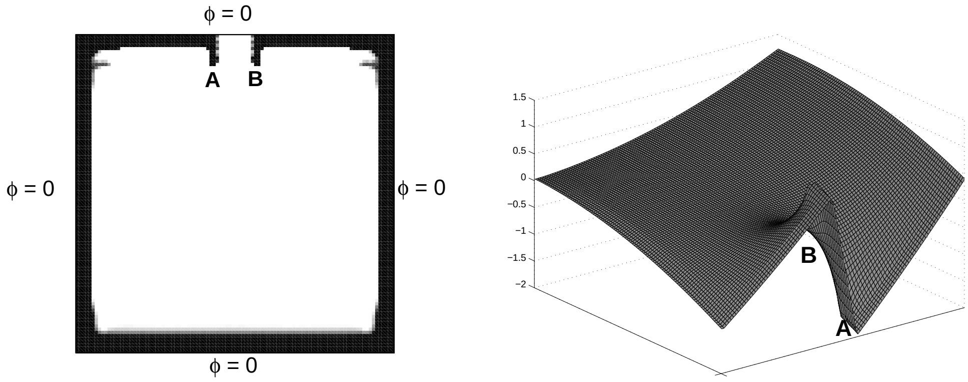

(a) Optimized design (b) Warping function

Figure 14: Optimized solution of Example 10

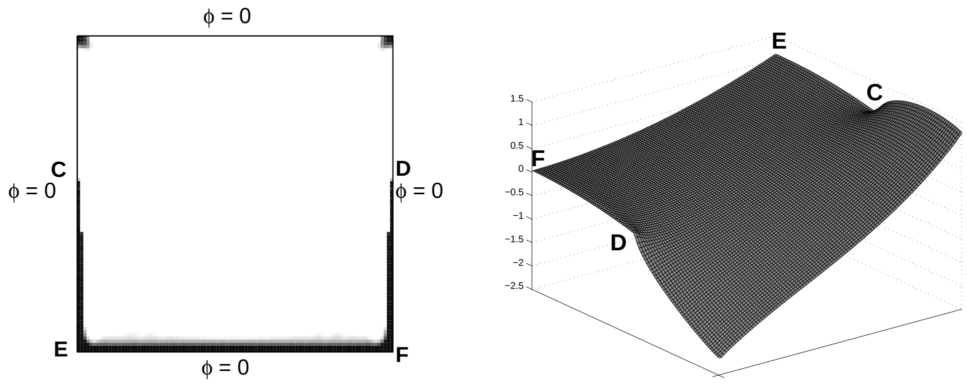

(a) Optimized design (b) Warping function

Figure 15: Optimized solution of Example 11

Acknowledgments: The major part of this work was performed during the first author stay at the Dep. of Mech. Eng., Technical University of Denmark. The authors are grateful to Krister Svanberg for supplying the MMA-optimization subroutines. The work has been supported by BFM2001-0738 (Spain), GC-02-001 (Spain) and through "the Phonon Project", Danish Technical Research Council.

References

[1] M.P. Bendsøe. Optimized shape design as a material distribution problem. Structural Optimization, 1:193–202, 1989.

[2] M.P. Bendsøe. Optimization of Structural Topology, Shape and Material. Springer, 1995.

[3] M.P. Bendsøe and O. Sigmund. Material interpolation schemes in topology optimization. Archive of Applied Mechanics, 69:635–654, 1999.

[4] M.P. Bendsøe and O. Sigmund. Topology Optimization: Theory, Methods and Applications. Springer, 2003.

[5] T. Burns and A.V. Cherkaev. Optimal distribution of multimaterial composites for torsional beams. Structural Optimization, 13(1):14–23, 1997.

[6] R.D. Cook, D.S. Malkus, M.E. Plesha, and R.J. Witt. Concepts and Applications of Finite Element Analysis. Wiley, 2002.

[7] J. Goodman, R.V. Kohn, and L. Reyna. Numerical study of a relaxed variational problem from optimal design. Computer Methods in Applied Mechanics and Engineering, 57:107–127, 1986.

[8] Y.Y. Kim and T.S. Kim. Multiobjective topology optimization of a beam under torsion and distortion. AIAA Journal, 40(2):376–381, 2002.

[9] A. Klarbring, J. Petersson, B. Torstenfelt, and M. Karlsson. Topology optimization of flow networks. Computer Methods in Applied Mechanics and Engineering, 192(35-36):3909–3932, 2003.

[10] Q. Li, G.P. Steven, O.M. Querin, and Y.M. Xie. Stress based optimization of torsional shafts using an evolutionary procedure. International Journal of Solids and Structures, 38:5561–5677, 2001.

[11] K.A. Lurie and A.V. Cherkaev. Nonhomogeneous bar of extremal torsional rigidity. In Nonlinear problems in structural mechanics. Structural Optimization. Naukowa Dumka, 1978.

[12] O. Sigmund. On the optimality of bone microstructure. In P. Pedersen and M.P. Bendsøe, editors, Synthesis in Bio Solid Mechanics, pages 221–234. IUTAM, Kluwer, 1999.

[13] O. Sigmund. A 99 line topology optimization code written in matlab. Structural and Multidisciplinary Optimization, 21(2), 2001.

[14] O. Sigmund. Design of multiphysics actuators using topology optimization - part i: One-material schemes. Computer Methods in Applied Mechanics and Engineering, 190:6605–6627, 2001.

[15] O. Sigmund and J. Petersson. Numerical instabilities in topology optimization: A survey on procedures dealing with checkerboards, mesh-dependencies and local minima. Structural and Multidisciplinary Optimization, 16(1):68–75, 1998.

[16] K. Svanberg. The method of moving asymptotes - a new method for structural optimization. Int. J. Numer. Meth. Engrg., 24:359–373, 1987.